



Lossy Ferrite Core-Dielectric Shell Structure for Miniature GHz Axial-Mode Helical Antenna

Woncheol Lee , Yang-Ki Hong , Hoyun Won , Minyeong Choi, Katelyn Isbell ,
Jaejin Lee, Tae-Wan Kim , and Seong-Ook Park 

Abstract—A lossy ferrite core/dielectric shell structure effectively miniaturizes an axial-mode helical antenna (AM-HA) without sacrificing the antenna gain in the range of 2.85–3.45 GHz. Co₂Z hexaferrite-glass composite was used as an inner core and acrylonitrile butadiene styrene as an outer shell. The volume of the AM-HA was reduced by 29% while maintaining realized gain of 9.0 dBi, compared to air-core AM-HA. The simulation also confirmed that further miniaturization of the AM-HA up to 43% is achievable with a slight decrease in realized gain from 9 to 8.7 dBi. The designed magnetic core/dielectric shell structure offers a vast selection of lossy ferrite for miniaturization of the AM-HA.

Index Terms—Axial-mode (AM), circular polarization, helical antenna (HA), material loading.

I. INTRODUCTION

THE axial-mode helical antennas (AM-HAs) have been attractive candidates for radar, satellite, unmanned aerial vehicle, and mobile systems due to their radiation characteristics such as endfire radiation and circular polarization [1], [2]. However, the large volume (V) of AM-HAs limits their use in various applications.

Numerous approaches have been proposed to reduce the V of AM-HA [2]–[8]. One method is based on antenna structure. The number of turns and pitch angle of the antenna radiator were optimized to miniaturize AM-HA [3]. Also, the hemispherical winding configuration of the radiator leads to a low-profile structure [4]. Furthermore, shapes of the radiator, such as a periodic sinusoidal patterned radiator and a double helical structured radiator, were proposed to reduce the V of the AM-HA [5], [6].

The other approach is the dielectric or magnetic core loading onto the center of the helical radiators [2], [7], [8]. In [7] and [8], the AM-HA shows the voltage standing-wave ratio of 2:1, axial ratio (AR) under 3 dB, and lower operational frequency by loading a high-dielectric material, indicating antenna miniaturization. However, the material with a high permittivity reduces

Manuscript received February 9, 2019; revised March 16, 2019; accepted March 17, 2019. Date of publication March 27, 2019; date of current version May 3, 2019. This work was supported by the E. A. “Larry” Drummond Endowment at the University of Alabama and EMW Co., Ltd. (Corresponding author: Yang-Ki Hong.)

W. Lee, Y.-K. Hong, H. Won, M. Choi, and K. Isbell are with the Department of Electrical and Computer Engineering, The University of Alabama, Tuscaloosa, AL 35487 USA (e-mail: wlee43@crimson.ua.edu; ykhong@eng.ua.edu; hwon@crimson.ua.edu; mchoi11@crimson.ua.edu; krisbell1@crimson.ua.edu).

J. Lee is with the Client Research and Development, Intel Corporation, Hillsboro, OR 97124 USA (e-mail: jaejin.lee@intel.com).

T.-W. Kim and S.-O. Park are with the Department of Electrical Engineering, Korea Advanced Institute of Science and Technology, Daejeon 34141, South Korea (e-mail: gold427@kaist.ac.kr; soparky@kaist.ac.kr).

Digital Object Identifier 10.1109/LAWP.2019.2906505

the 3-dB AR bandwidth ($AR_{3dB, BW}$) [7]. It was reported that the loading of a Z-type Co₂Z hexaferrite-glass composite (Co₂Z-HGC) core reduces 82% of the V of AM-HA antenna [2]. The V reduction is due to the contribution of both relative permittivity (ϵ_r) and permeability (μ_r) of the ferrite to the miniaturization factor ($n = (\epsilon_r \cdot \mu_r)^{0.5}$) [2]. However, the realized gain (RG) of the ferrite core (FC)-loaded AM-HA (FC-AM-HA) significantly decreased from 8.8 to 0.5 dBi due to the magnetic loss, i.e., the magnetic loss tangent ($\tan\delta_\mu = 0.08$) of the FC. We have also reported that the antenna radiation efficiency (RE) increases to 77% from 66% with the decrease of $\tan\delta_\mu$ of the ferrite substrate from 0.11 to 0.05 [9]. The extrapolation of experimental data suggests that the RE of 86% is achievable at 0.01 of $\tan\delta_\mu$. However, a ferrite is magnetically lossy at the ultrahigh frequency due to the ferromagnetic resonance [10], [11]. A low $\tan\delta_\mu$ of 0.05 with the μ_r of 2.1 at 2.2 GHz was reported [10], but is still too high to apply to the antenna. Therefore, there is a limited selection of ferrites for GHz antenna design.

In this letter, we report a lossy-ferrite-core/dielectric-shell (LFC-DS) structure that miniaturizes an AM-HA and retains a reasonable antenna gain even with a high $\tan\delta_\mu$. This structure offers a vast selection of ferrites for GHz AM-HA design. The LFC-DS cylinder is composed of an inner Co₂Z-HGC core and outer dielectric shell (DS). Antenna simulation was performed on four types of AM-HAs, namely air-core (AC)-, FC-, DC-, and LFC-DS-AM-HA using ANSYS High-Frequency Structure Simulator (HFSS ver. 18). To validate the simulated results, AC- and LFC-DS-AM-HA were fabricated and characterized.

II. ANTENNA DESIGN AND SIMULATION

Four types of the AM-HA were designed and simulated for antenna performance. The radiator of AC-AM-HA was helically wound counterclockwise with three turns with a uniform conductor diameter (d_c) of 0.812 mm. A typical AM-HA has an impedance of 140 Ω [12]. Likewise, our simulation confirmed that the impedance of the designed AC-AM-HA is about 150 Ω beyond 2.8 GHz. Thus, the quarter-wave-like transmission line (QTL) was designed to match the impedance to 50 Ω as shown in Fig. 1(a). The QTL was printed on an FR4 epoxy substrate ($\epsilon_r = 4.4$, dielectric loss tangent ($\tan\delta_\epsilon$) = 0.02, thickness = 1.5 mm). The ground plane is located at the bottom of the substrate. The detailed dimensions of the AC-AM-HA are given in Table I.

Fig. 1(b) shows an FC-AM-HA for the study of the effects of dynamic properties of the core on antenna performance. For the antenna performance simulation, the following arbitrary ϵ_r and μ_r of the core have been chosen: core 1: $\epsilon_r = 1$ and $\mu_r = 1$ ($n = 1$); core 2: $\epsilon_r = 4$ and $\mu_r = 1$ ($n = 2$); core 3:

TABLE I
DETAILED DESIGN PARAMETERS FOR THE HELICAL ANTENNA

r_{GND}	w_1	w_2	α	d_c	r_h	s
50 mm	2.9 mm	1.04 mm	57.3°	0.812 mm	13.4 mm	23 mm

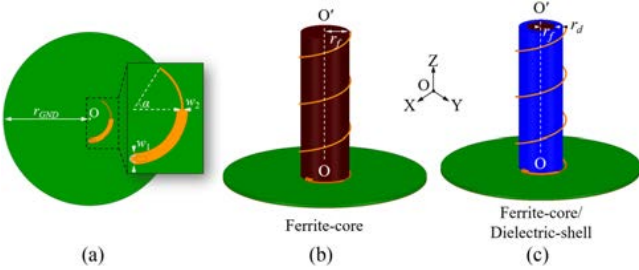


Fig. 1. Dimensions and geometry of (a) an AM-HA (top view) and helical antenna with (b) ferrite-core and (c) ferrite-core/dielectric-shell.

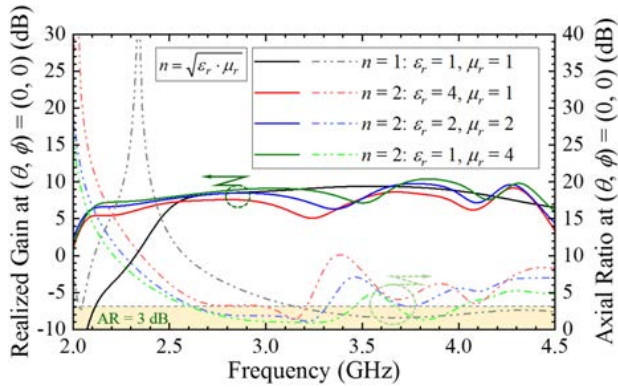


Fig. 2. Simulated frequency-dependent realized gain (RG_{00}) and AR at boresight (AR_{00}) of a helical antenna with different core material properties.

$\epsilon_r = 2$ and $\mu_r = 2$ ($n = 2$); and core 4: $\epsilon_r = 1$ and $\mu_r = 4$ ($n = 2$). The $\tan\delta_\epsilon$, $\tan\delta_\mu$, and radius of the core were fixed to 0.01, 0.01, and 12 mm, respectively. Fig. 2 shows the simulated frequency-dependent RG and the AR at boresight [$(\theta, \phi) = (0, 0)$] of AM-HA with the different cores, i.e., different ϵ_r and μ_r . The first crossing frequencies of the AR at boresight (AR_{00}) under 3 dB ($f_{AR00=3dB}$) of the AM-HA with the cores 2, 3, and 4 are lower than the $f_{AR00=3dB}$ of the AM-HA with the core 1, indicating antenna miniaturization. The AR_{3dB_BW} decreases as the ϵ_r increases, and the AM-HA with the core 4 shows the widest AR_{3dB_BW} . Contrarily, the RG at the boresight (RG_{00}) increases as the μ_r of the core increases. All cored AM-HA show a good impedance matching (reflection coefficient (Γ) < -10 dB) from 2.5 to 4 GHz (not shown here). Accordingly, an FC loading can be more effective than a dc loading in AM-HA miniaturization, while exhibiting a good antenna performance.

For the realistic simulation, the measured dynamic properties of the Co_2Z -HGC core ($\mu_r = 2$, $\tan\delta_\mu = 0.1$, $\epsilon_r = 7$, and $\tan\delta_\epsilon = 0.01$) were used. The same helical radiator and feeding structure in Fig. 1(a) with the radius of the FC (r_f) of 12 mm were also used. Fig. 3 shows the simulated frequency-dependent radiation performance of the AC-AM-HA and FC-AM-HA. The loading of the FC shifts the first crossing frequency of the 10 dB return loss to 1.88 from 2.45 GHz (not shown here)

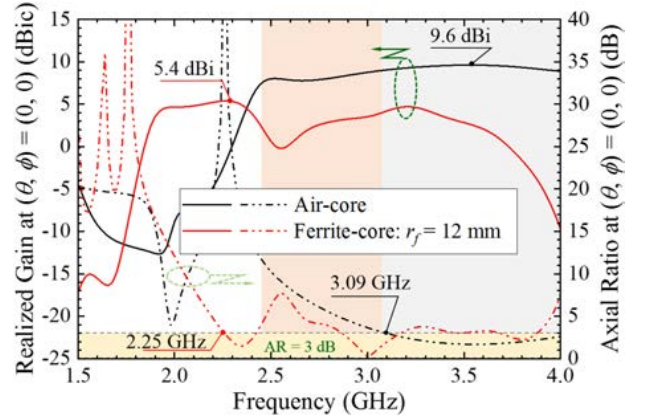


Fig. 3. Simulated antenna performance of AC- and FC-AM-HA: frequency-dependent RG_{00} and AR_{00} .

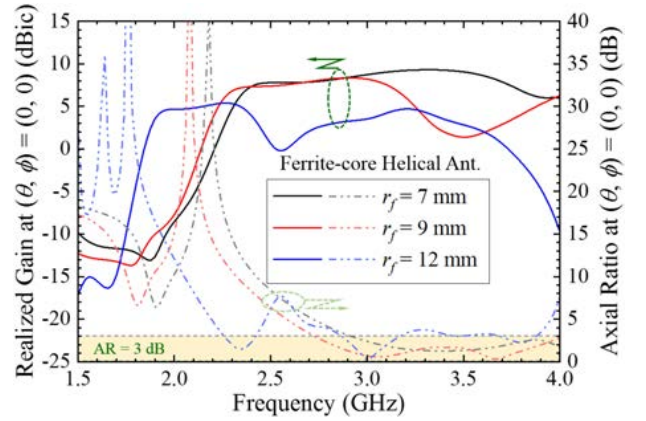


Fig. 4. Simulated frequency-dependent RG_{00} and AR_{00} of the FC-AM-HA with different radius of ferrite-core (r_f).

and $f_{AR00=3dB}$ to 2.25 from 3.09 GHz, but the maximum RG_{00} (RG_{00_max}) of the AC-AM-HA decreased from 9.6 to 5.4 dBic, which is undesired.

Therefore, we have performed a parametric study of the r_f to observe its effect on antenna performance. The results show that the RG_{00_max} of the FC-AM-HA increased from 5.4 to 9.4 dBic as the r_f decreases from 12 to 7 mm as shown in Fig. 4. Although the FC-AM-HA with the r_f of 7 mm showed similar RG_{00_max} to the AC-AM-HA, the $f_{AR00=3dB}$ of FC-AM-HA shifted from 2.25 ($r_f = 12$ mm) to 2.91 GHz ($r_f = 7$ mm). By comparing with the $f_{AR00=3dB}$ of AC-AM-HA, the $f_{AR00=3dB}$ of FC-AM-HA ($r_f = 7$ mm) shifted to a lower frequency by only 180 MHz, indicating insufficient antenna miniaturization.

Thus, here, we propose a lossy-ferrite-core/dielectric-shell (LFC-DS) AM-HA in Fig. 1(c) to miniaturize AM-HA with minimal antenna gain loss. The LFC-DS structure consists of inner Co_2Z -HGC core and outer acrylonitrile butadiene styrene (ABS) shell. Measured $\mu_r = 2$, $\tan\delta_\mu = 0.1$, $\epsilon_r = 7$, and $\tan\delta_\epsilon = 0.01$ of Co_2Z -HGC and $\epsilon' = 2$ and $\tan\delta_\epsilon = 0.01$ of ABS were used in the simulation. Fig. 5(a) shows the RG_{00} and AR_{00} of LFC-DS-AM-HA with different r_f when the outer radius of ABS-shell (r_d) is set to 11 mm. The ratio of ferrite to dielectric material ($a_{fd} = r_f^2/r_d^2$) is 0.40, 0.52, and 0.67. As the r_f increases from 7 to 9 mm, the $f_{AR00=3dB}$ decreases from 2.84 to 2.68 GHz,

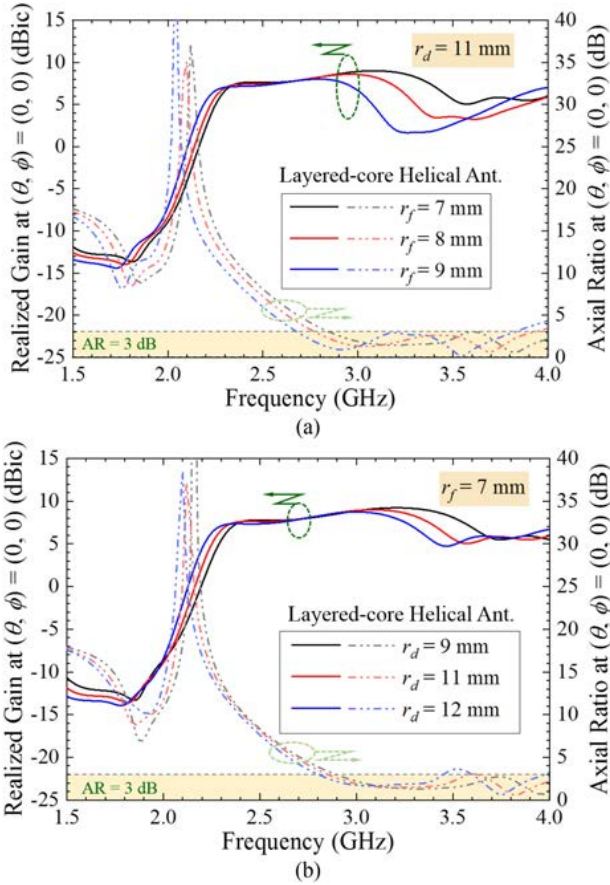


Fig. 5. Simulated frequency-dependent RG_{00} and AR_{00} of the LFC-DS-AM-HA with various radius of (a) ferrite (r_f) and (b) ABS (r_d).

while the RG_{00_max} decreases from 9 to 8 dBic. Fig. 5(b) shows the RG_{00} and AR_{00} of LFC-DS-AM-HA with different r_d when the r_f is 7 mm for a_{fd} of 0.60, 0.40, and 0.34. The $f_{AR00=3dB}$ shifted from 2.89 to 2.8 GHz, while the RG_{00_max} decreases from 9.2 to 8.7 dBic with an increase of r_d from 9 to 12 mm. The optimal value of r_d and r_f for the LFC-DS-AM-HA was chosen to be 11 and 7 mm, respectively.

To explain the origin of high RG_{00} by loading the LFC in contrast with the FC loading, a vector magnetic field distribution of FC- and LFC-DS-AM-HA is presented in Fig. 6. The magnetic flux in the light brown region (ferrite region) for FC-AM-HA is less rotated as compared to magnetic flux in the light green region (ABS-shell region) for LFC-AM-HA. Therefore, the magnetic flux in the FC lags behind the magnetic field generated by the alternating current on the helical coil. This lagging represents the energy loss due to the magnetic loss of the FC [13]. Accordingly, the ABS-shell mitigates RG_{00} degradation near the region where the magnetic fields changes dramatically with high magnitude. That is, the LFC-DS-AM-HA is less vulnerable to the magnetic loss of the ferrite.

To quantify the antenna V reduction by LFC-DS loading, the AC-AM-HA of 55 cm^3 ($r_h = 14.6$ mm and $s = 27.4$ mm) was designed and simulated for antenna performance. The simulated frequency-dependent RG_{00} and AR_{00} of AC-AM-HA with the V of 55 cm^3 are compared with those of LFC-DS-AM-HA ($r_h = 13.4$ mm, $s = 23$ mm, $r_d = 11$ mm, and $r_f = 7$ mm) in Fig. 7. For both antennas, the $f_{AR00=3dB}$ appears at 2.84 GHz,

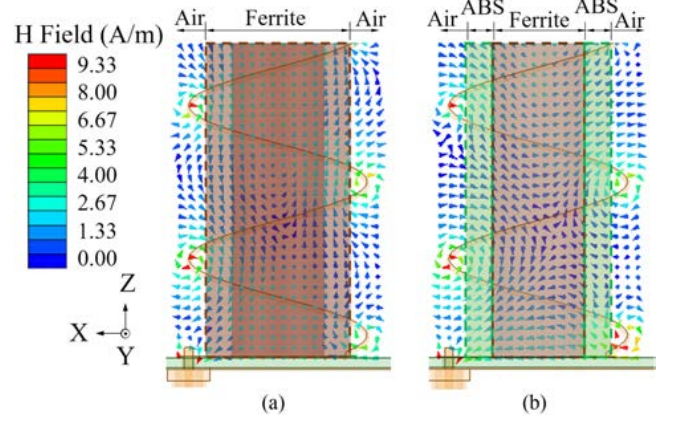


Fig. 6. Cross-sectional vector magnetic field distribution for (a) FC-AM-HA ($r_d = 11$ mm) and (b) LFC-DS-AM-HA ($r_d = 11$ mm and $r_f = 7$ mm).

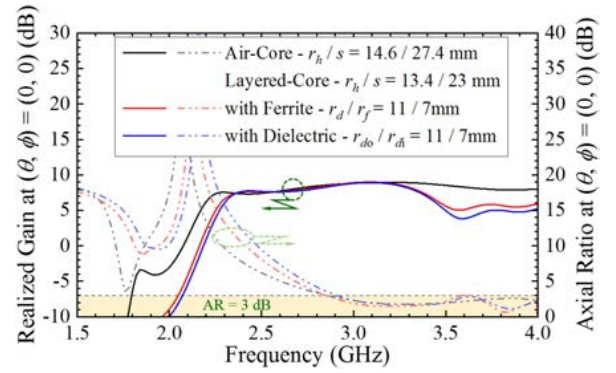


Fig. 7. Simulated frequency-dependent RG_{00} and AR_{00} of the air- ($r_h = 14.6$ mm and $s = 27.4$ mm) and LFC-DS ($r_h = 13.4$ mm, $s = 23$ mm) with ferrite inner-core ($r_d = 11$ mm and $r_f = 7$ mm) and dielectric ($\epsilon_r = 14$) outer-shell ($r_{do} = 11$ mm and $r_{di} = 7$ mm) helical antennas.

and the RG_{00_max} is 9 dBic. Accordingly, the V of the AM-HA was reduced by 29% (from 55 to 38.9 cm^3) by loading the LFC-DS with r_d of 11 mm and r_f of 7 mm. Further V reduction of 43% is achievable by loading the LFC-DS with r_d and r_f of 12 and 7 mm, respectively, with a slight decrease in RG_{00_max} of 0.3 dBic (not shown here). To compare the dielectric loading effectiveness in the V reduction with the ferrite loading, the inner LFC of LFC-DS-AM-HA was replaced with a dc with ϵ_r of 14. The simulation results show that a dielectric-core-loaded AM-HA (DC-AM-HA) showed 0.07 GHz higher $f_{AR00=3dB}$ and 0.1 dBic lower RG_{00_max} than those of the LFC-DS-AM-HA. Based on this result, it can be concluded that the LFC-DS structure with the inner LFC helps to decrease the V of the AM-HA at the minimum expense of RG even with the high $\tan\delta_\mu$ of 0.1 while obtaining broader AR_{3dB_BW} than the DC with high ϵ_r . Experiments in Section III have confirmed simulation results.

III. ANTENNA FABRICATION AND MEASURED RESULTS

In order to verify the effectiveness of the LFC loading in the V reduction and antenna performance, we have fabricated AC- and LFC-DS-AM-HA according to the parameters used in our parametric study shown in Fig. 7. A 20 AWG copper wire (diameter = 0.812 mm) was helically wound in counterclockwise with

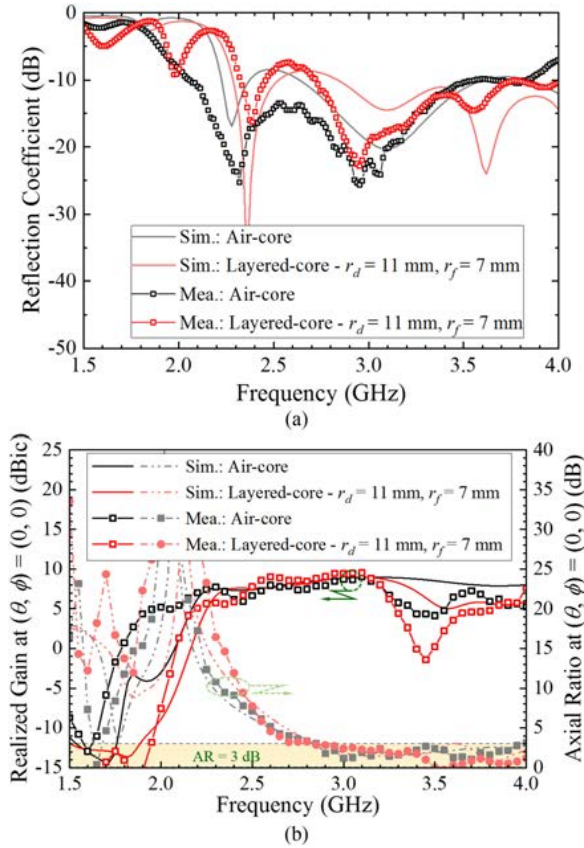


Fig. 8. Simulated and measured frequency-dependent (a) reflection coefficient and (b) RG_{00} and AR_{00} of the AC- and LFC-DS-AM-HA.

three turns. The QTL was formed on a double-sided copper-clad laminate FR-4 epoxy substrate with precision milling machines (LPKF ProtoMat S62). Then, a 50Ω SMA connector was used to feed antennas. The Co_2Z -HGC powder was prepared with the synthetic process in [14] for the inner LFC. The powder was then pressed into a cylinder and sintered. The radius of the prepared FC was 7 mm. For dielectric outer-shell preparation, a hollow cylinder with outer and inner radius of 11 and 7 mm, respectively, was printed with a 3-D printer (HICTOP 3DP-12) and ABS filament. The filament was extruded and deposited onto the test platform when the platform and nozzle were heated up to 110°C and 240°C , respectively. Then, the printed ABS-shell was cooled at room temperature for 10 min. After cooling, the LFC was inserted into the hollow structured ABS-shell. The fabricated antenna was characterized with a vector network analyzer (VNA: Agilent N5230) for scattering parameters and an in-lab anechoic chamber (Raymond EMC QuietBox AVS 700) with a linearly dual-polarized horn antenna for antenna radiation pattern. The AR of the fabricated antennas were calculated from the measured data [15].

Fig. 8 shows the measured antenna performance of the fabricated AC- and LFC-DS-AM-HA. Reasonable agreement between the measured and simulated results are observed. The slight discrepancy between results can be attributed to the fabrication tolerance and measurement errors. The $f_{AR00=3dB}$ of AC- and LFC-DS-AM-HA is 2.84 GHz. As for AR_{3dB_BW} , reasonably good impedance matching was observed from both fabricated AC- and LFC-DS-AM-HA. The RG_{00_max} of LFC-DS-AM-HA within the AR_{3dB_BW} is 9.5 dBic, which is 0.5 dBic

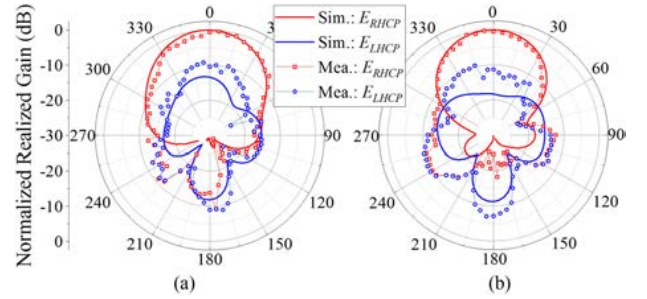


Fig. 9. Simulated and measured NRPs of (a) AC-AM-HA and (b) LFC-DS-AM-HA.

TABLE II
COMPARISON ON ANTENNA PERFORMANCE AMONG AM-HA

Name	Volume [cm ³]	$f_{AR00=3dB}$ [GHz]	AR_{3dB_BW} [MHz]	Max. RG_{00} [dBic]
AC-AM-HA (Sim/Exp)	55	2.84/2.84	1160/1160	9.0/9.0
FC-AM-HA (Sim)	38.9	2.25	690	5.4
DC-AM-HA (Sim)	38.9	2.91	1090	8.9
LFC-DS-AM-HA (Sim/Exp)	38.9	2.84/2.84	1160/1160	9.0/9.5

higher than the RG_{00_max} of AC-AM-HA. The results indicate that the antenna is miniaturized by loading the LFC-DS structure without RG degradation. Fig. 9 shows the measured and simulated far-field normalized radiation patterns (NRPs) at 2.9 GHz for AC-AM-HA and LFC-DS-AM-HA. The measured and simulated NRP for copolarization agree well, but are slightly different for cross polarization. This might be attributed to the small size of the chamber, causing some reflections. Both fabricated antennas showed the directional radiation pattern along the axis of the helical radiator. Additionally, both antennas showed the cross-polarization level of nearly -10 dB at boresight. Antenna performance and V are given in Table II. Here, we conclude that the LFC-DS-AM-HA outperforms the other AM-HAs.

IV. CONCLUSION

A volume reduction of an AM-HA by an LFC-DS, which consists of inner FC and outer DS, is demonstrated. The volume of AM-HA was reduced by 29% while maintaining a good antenna realized gain of 9.0 dBic even with the high magnetic loss of the FC (magnetic loss tangent of 0.1). Also, further volume reduction is achievable by increasing the volume of the inner FC. In general, ferrite is intrinsically lossy above 1 GHz. However, we have demonstrated that the LFC-DS structure offers a vast selection of ferrite for the volume reduction of AM-HA by overcoming the lossy characteristics of ferrite above 1 GHz. The LFC-DS structure will be further investigated for its applications at frequencies above 3 GHz and compared with the normal mode helical antenna.

ACKNOWLEDGMENT

The authors would like to thank L. Vanderburgh for antenna fabrication.

REFERENCES

- [1] L. Liu, Y. Li, Z. Zhang, Z. Feng, "Circularly polarized patch-helix hybrid antenna with small ground," *IEEE Antennas Wireless Propag. Lett.*, vol. 13, pp. 361–364, 2014.
- [2] N. Neveu, Y.-K. Hong, J. Lee, J. Park, G. S. Abo, W. Lee, and D. Gillespie, "Miniature hexaferrite axial-mode helical antenna for unmanned aerial vehicle applications," *IEEE Trans. Magn.*, vol. 49, no. 7, pp. 4265–4268, Jul. 2013.
- [3] H. Nakano, H. Takeda, T. Honma, H. Mimaki, and J. Yamauchi, "Extremely low-profile helix radiating a circularly polarized wave," *IEEE Trans. Antennas Propag.*, vol. 39, no. 6, pp. 754–757, Jun. 1991.
- [4] H. T. Hui, K. Y. Chan, and E. K. N. Yung, "The low-profile hemispherical helical antenna with circular polarization radiation over a wide angular range," *IEEE Trans. Antennas Propag.*, vol. 51, no. 6, pp. 1415–1418, Jun. 2003.
- [5] A. H. Safavi-Naeini and O. Ramahi, "Miniaturizing the Axial Mode Helical Antenna," in *Proc. IEEE Conf. Commun. Electron.*, Jun. 2008, pp. 374–379.
- [6] I. Ghoreishian and A. Safaai-Jazi, "A new doubly helical antenna," *Micro. Opt. Technol. Lett.*, vol. 57, no. 10, pp. 2351–2355, Oct. 2015.
- [7] T. A. Latef and S. K. Khamas, "Measurement and analysis of a helical antenna printed on a layered dielectric hemisphere," *IEEE Trans. Antennas Propag.*, vol. 59, no. 12, pp. 4831–4835, Dec. 2011.
- [8] W. Coburn, C. Ly, T. Burcham, R. Harris, and A. Bamba, "Design and fabrication of an axial mode helical antenna," *Appl. Comput. Electromagn. Soc. J.*, vol. 24, no. 6, pp. 559–566, Dec. 2009.
- [9] W. Lee, Y.-K. Hong, J. Lee, D. Gillespie, K. G. Ricks, F. Hu, and J. Abu-Qahouq, "Dual-polarized hexaferrite antenna for unmanned aerial vehicle (UAV) applications," *IEEE Antennas Wireless Propag. Lett.*, vol. 12, pp. 765–768, 2013.
- [10] W. Lee, Y.-K. Hong, M. Choi, H. Won, J. Lee, G. LaRochelle, and S. Bae, "Figure of merit of W-type $\text{BaCo}_{1.4}\text{Zn}_{0.6}\text{Fe}_{16}\text{O}_{27}$ hexaferrite for gigahertz device applications," *IEEE Magn. Lett.*, vol. 8, 2017, Art. no. 5109204.
- [11] W. Lee, Y.-K. Hong, J. Park, G. LaRochelle, and J. Lee, "Low-loss Z-type Hexaferrite ($\text{Ba}_3\text{Co}_2\text{Fe}_{24}\text{O}_{41}$) for GHz Antenna Applications," *J. Magn. Mater.*, vol. 414, pp. 194–197, Sep. 2016.
- [12] J. D. Kraus, "A 50-Ohm input impedance for helical beam antennas," *IEEE Trans. Antennas Propag.*, vol. AP-25, no. 6, p. 913, Nov. 1977.
- [13] B. D. Cullity and C. D. Graham, *Introduction to Magnetic Materials*, 2nd ed., Hoboken, NJ, USA: Wiley, 2009, p. 417.
- [14] J. Lee, Y.-K. Hong, S. Bae, J. Jalli, and G. S. Abo, "Low loss Co_2Z ($\text{Ba}_3\text{Co}_2\text{Fe}_{24}\text{O}_{41}$)-glass Composite for gigahertz antenna application," *J. Appl. Phys.*, vol. 109, 2011, Art. no. 07E530.
- [15] C. A. Balanis, *Antenna Theory: Analysis and Design*, 3rd ed., Hoboken, NJ, USA: Wiley, 2005.